Structure and Properties of Low Molecular Weight Amphiphilic Peptide Hydrogelators

ARTICLE *in* THE JOURNAL OF PHYSICAL CHEMISTRY B · JANUARY 2008

Impact Factor: 3.3 · DOI: 10.1021/jp076495x · Source: PubMed

4 AUTHORS, INCLUDING:

Rajendra Narayan Mitra
University of North Carolina at Chapel Hill
19 PUBLICATIONS **425** CITATIONS
SEE PROFILE

Debapratim Das
Indian Institute of Technology Guwahati
23 PUBLICATIONS **628** CITATIONS
SEE PROFILE

Structure and Properties of Low Molecular Weight Amphiphilic Peptide Hydrogelators

Rajendra Narayan Mitra, Debapratim Das, Sangita Roy, and Prasanta Kumar Das*,†

Department of Biological Chemistry, Indian Association for the Cultivation of Science, Jadavpur, Kolkata 700 032, India

Received: August 13, 2007; In Final Form: September 24, 2007

The search for low molecular weight hydrogelators (LMWH) with varying structural motif is getting intense because of its potential application in the field of biomedicines as well as the diversified area of nanobiotechnology. In this paper, we have developed hydrogels of simple cationic dipeptide amphiphiles (**1**−**6**) that have a wide range of minimum gelation concentration (MGC), 12−0.25% (w/v) in plain water. The self-aggregation behavior of these thermoreversible hydrogelators has been investigated through different spectroscopic and microscopic techniques. A balanced participation of hydrophilicity and hydrophobicity is the major driving force for gelation, which could be modulated by a minute change in the architecture of the amphiphile head. The prospective use of this material in controlled release suggests that this system could also be applied as the drug delivery vehicle. Moreover, the presence of a biodegradable amide linkage susceptible to base or enzyme-catalyzed hydrolysis increases its probable applications as biomaterials.

Introduction

Hydrogel, a class of soft materials, is rapidly expanding in the field of material science due to its high potential in wide-ranging applications including biotechnology. Hydrogels are mostly made from high molecular weight natural polymers[1−3] (collagens, polysaccharides) and also from hydrophilic synthetic polymers[4,5] (poly(acrylic acid) and derivatives and polypeptides). While nonpolymeric low molecular weight hydrogelators (LMWH) are less abundant, drawing considerable attention in soft material research for the past couple of decades.[6−10] The supramolecular hydrogels made of low molecular weight gelators (LMWG) are at the center of focus due to their rapid response to external stimuli, thermoreversible nature, and possible biodegradability.[11−25] The noncovalent forces such as electrostatic attraction, $\pi-\pi$ stacking, dipole−dipole, and hydrogen bonding interactions clutch the LMWG molecules together and thus render many advantages over polymer gels. Despite the limited understanding of all the interactions that play a role, one can nevertheless try to design new gelators for plain water. Tuning the structure of the gelators can change efficiencies, stability, and properties of gelation. To date, the composite of molecular self-assembly leading to gelation in water includes sugar-based gelators, bis-urea carboxylate derivatives, bis-oxalyl amides, and tartarate-based gemini surfactants.[19] It appears that there is often a very delicate balance between structure, intermolecular interactions, and gelating properties. Thus, rational designing of new, effective, small-molecule gelators is a difficult task for chemists. At this point, it is indispensable to acquire knowledge about the water immobilization mechanism and the effect of different structural motifs on the gelating ability of such LMWGs. To utilize them in biomedicinal and biological applications, development of LMWG that have the ability to immobilize simple water molecules in the absence of any other additives is also important.

In this paper, we report hydrogelation of cationic dipeptide amphiphiles (**1**−**6**, Scheme 1) with a wide range of gelation (12−0.25%, w/v, minimum gelation concentration (MGC)) in plain water. Amino acid based compounds are potent candidates to be gelators because of inherent biocompatibility leading to their application in the biomedicinal arena. Investigation directed toward the influence of head group tuning of the amphiphiles on the stability and gelation properties, including supramolecular arrangements in the aggregated structure, led to the development of efficient gelartors **5** and **6**, which also showed controlled drug releasing ability. The results on hydrogelation study provide understanding at the molecular level on the basic structural requirements in designing efficient amphiphilic hydrogelators.

Experimental Section

Materials. Silica gel of 60−120 mesh, L-tryptophan, L-phenylalanine, l-proline, *n*-hexadecylamine, *N*,*N*-dicyclohexylcarbodiimide (DCC), 4-*N*,*N*-(dimethylamino)pyridine (DMAP), *N*-hydroxybenztriazole (HOBT), iodomethane, solvents, and all other reagents were procured from SRL, India. Water used throughout the study was Milli-Q water. Thin-layer chromatography was performed on Merck precoated silica gel 60-F_{254} plates. All the deuterated solvents for NMR experiments and 8-anilino-1-naphthalenesulphonic acid (ANS) were obtained from Aldrich Chemical Co. Amberlyst A-26 chloride ion-exchange resin was obtained from BDH, U.K. Mass spectrometric (MS) data were acquired by electron spray ionization (ESI) technique on a Q-tof-Micro Quadruple mass spectrophotometer, Micromass.

Preparation of Hydrogel. The aqueous dispersions of the required amount of compounds **1**−**6** were slowly heated to dissolve the compounds in water and then allowed to cool slowly (undisturbed) to room temperature in a vial with i.d. = 10 mm. After 20−30 min the solid aggregate mass was stable to inversion of the glass vial when the glass vial was turned upside down; the compound was recognized to form a hydrogel.

Determination of Gel-Sol Transition Temperature (T_{gel}). The gel to sol transition temperature (T_{gel}) was determined by

* To whom correspondence should be addressed. Fax: +(91)-33-24732805. E-mail: bcpkd@iacs.res.in.
† Also at Centre for Advanced Materials, Indian Association for the Cultivation of Science.

10.1021/jp076495x CCC: $37.00
Published on Web 12/04/2007

SCHEME 1: Chemical Structures of the Peptide Amphiphiles, 1−6

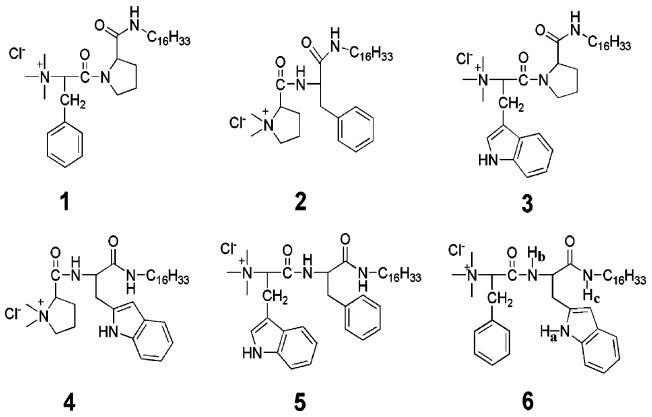

placing a hydrogel containing an inverted screw-capped glass vial with i.d. = 10 mm in a thermostatted oil bath, and then the temperature was raised at a rate of 2 °C/min. Here, the T_{gel} was defined as the temperature (±0.5 °C) at which the hydrogel melts and starts to flow out of the gel.

Microscopic Studies. Scanning electron microscopy (SEM) and transmission electron microscopy (TEM) measurements were performed on JEOL-6700F and JEOL JEM 2010 microscopes, respectively. A piece of gel was mounted on a glass slide and a 300-mesh carbon-coated copper grid for SEM and TEM sampling, respectively, and dried for few hours under vacuum before imaging. For bright-field and fluorescence microscopic images of the gels at MGC, the following method was used: a small quantity of gel was placed on a microscope slide, which was sealed with a glass coverslip, and images were taken. Fluorescence microscopy was conducted using a light microscope (BX61, Olympus) equipped with a filter set consisting of a BP330-385 nm for an exciter and a band absorbance filter covering wavelengths below 420 nm.

Circular Dichroism. The circular dichroism (CD) spectra of **6** with concentration variation (from 0.005 to 0.05%, w/v) at room temperature and with varying temperatures (from 40 to 90 °C) at 0.05%, w/v aqueous solution, were recorded by using a quartz cuvette of 1 mm path length with a Jasco J-815 spectropolarimeter.

NMR Experiment. ^{1}H NMR and 2D-NOESY spectra were recorded on an AVANCE 300 MHz (Bruker) spectrometer.

Fluorescence Spectroscopy. The emission spectra of ANS were recorded on a Varian Cary Eclipse fluorescence spectrophotometer by adding the probe molecules in aqueous solutions of transparent hydrogels, i.e., **2** and **4**−**6** gels with varying concentrations at room temperature. ANS was initially dissolved in MeOH, and from this super stock the required amount of ANS solution was added to the experimental solutions [5 μL of super stock (0.01 M) was added to a 5 mL aqueous solution of the gelators to reach the probe concentration of 1×10^{-5} M]. The ANS solutions were excited at $\lambda_{ex} = 365$ nm.

FTIR Measurements. FTIR measurements of the gelators in $CHCl_3$ solution and dried gel from D_2O were carried out in a Shimadzu FTIR-8100 spectrophotometer using a 1 mm KBr cell and silicon wafer, respectively, at the MGC values.

Controlled Release of Entrapped Vitamin B_6 andB_{12} from Hydrogel. The controlled release of entrapped biomolecules was carried out as follows: 0.2 mL of 2 mM vitamin solutions (vitamin B_6 and B_{12}) in pH 7.0 phosphate buffer (1 mM) was added to 0.5 and 3.0% (w/v) gelators in different vials, heated to their T_{gel}, and held for a few hours undisturbed to attain the gel state at room temperature. Then, a 0.2 mL, pH 7.0 phosphate buffer (1 mM) solution was added on top of each gel. The 0.2 mL supernatant buffer solution was removed each time, and the concentrations of the released vitamins were analyzed by time-dependent UV−vis spectra using a Shimadzu UV-1700 analyzer. The release rate of vitamins was investigated in triplicate at room temperature.

TABLE 1: Gelation Test Results of 1−6 in Plain Water

gelator	state[a]	MGC (%, w/v)	T_{gel} (°C) at MGC
1	OG	12	42
2	TG	10	44
3	OG	7	46
4	TG	3	52
5	TG	0.4	56
6	TG	0.25	60

[a] OG, opaque hydrogel; TG, transparent hydrogel.

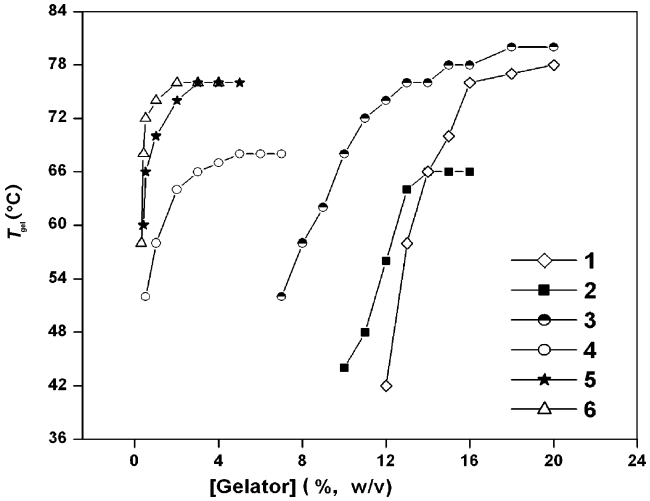

Figure 1. Variation of the gel to sol transition temperature (T_{gel}) with the gelator concentrations.

Results and Discussion

Gelation ability of LMWG primarily depends on its molecular architecture, which gets focused at the head group when the process is induced from a surfactant.[21,26,27] In the present study, the hydrogelation ability of six dipeptide based amphilphiles (**1**−**6**) was tested by the "stable-to-inversion of the container" method (Table 1).[28−30] In our previous study,[31] the aqueous self-assemblies of **2** and **4** were utilized as a template for asymmetric transformation at significantly lower concentration (~0.3%, w/v) with respect to their MGC. While no gelation was observed for **6** at ~0.3% (w/v) due to stirring, induced mechanical agitation that breaks up the weak 3D network within the physical gel. However, a detailed study leads to the development of hydrogels where MGC (Table 1) steadily decreased from **1** to **6** with concurrent increase in T_{gel}.

In concurrence with the literature, the increase of T_{gel} with the gelator concentration (Figure 1)[28−30] and also low MGC indicate that self-assembly in the gel state is driven by strong intermolecular noncovalent interaction. Correlation between MGC and the head group structure of the gelators specifies that the presence of a planar aromatic ring in the interior of the gelator head (**1** vs **2**; **3** vs **4**) improves the hydrogelation efficiency presumably due to better $\pi-\pi$ stacking. In contrast, a rigid/strained proline moiety at the interior of **1** and **3** possibly hinders the supramolecular arrangement resulting the formation of opaque gels with an increase in MGC and decrease in T_{gel}.

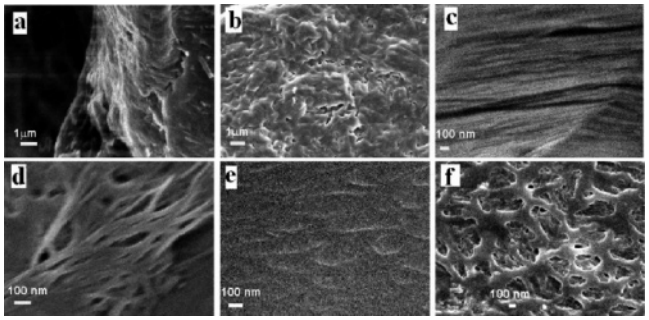

Figure 2. (a−f) FE-SEM images of the dried samples of **1**−**6** at MGC.

Moreover, when an extended aromatic ring (in tryptophan) is used as the planar moiety (**1** to **3**; **2** to **4**), water gelation improves (lower MGC, Table 1) with higher thermal stability (Figure 1). These results illustrate that the incorporation of the planner aromatic ring at the gelator head group improves its gelation efficiency. The preceding results helped us to design two efficient hydrogelators **5** and **6** having planar moieties both at the interior and end of the surfactant head. Here, too, the extended aromatic moiety present in the interior of the head group yields the most efficient hydrogelator **6**. Hence, molecular level tuning of amphiphiles notably influences their gelation properties. The weak gelator **1** and efficient gelator **6** can immobilize 261 and 14 620 water molecules/gelator molecule, respectively, at MGC. All gels except **1** and **3** displayed good stability over a period of 1 year at room temperature.

Microscopic Studies. Supramolecular arrangement of **1**−**6** at the MGC was investigated with the field emission scanning electron microscopy (FESEM, Figure 2a−f). In continuation with the observed trend in MGC with head group structure, the opaque gel of **1** showed a lamellar fibrous morphophology (Figure 2a), while the transparent hydrogel of **2** formed an entangled fibrous network capable of entrapping more water molecules (Figure 2b). This difference in the 3D network again can be attributed to the localization of the planar aromatic moiety within the gelator molecule. A similar phenomenon was observed for **3** and **4**, where the opaque gel of **3** showed lamellar fibrous morphophology (∼300 nm, Figure 2c), and the later consisted of an intertwined fibrous 3D matrix with a diameter in the range of 100−200 nm (Figure 2d). Such a supramolecular network clearly delineates the reason for better water gelation efficiency of **2** and **4** compared to that of **1** and **3**, respectively. As expected from MGC values, efficient gelators **5** and **6** comprising planar moieties, at both the interior and the surfactant head, form a distinct porous interconnected 3D network with a dimension 60−75 nm that can hold more water due to its greater void volume (Figure 2e−f). Furthermore, high-resolution transmission electron micrograph (HRTEM) of **6** also supports porosity in its network (Figure S1, Supporting Information) with the width of ∼40 nm. Such supramolecular arrangement in the gel state of **4**−**6** was further supported by optical and fluorescence microscopic study (Figure 3) since they contain a tryptophan unit within the molecule itself that has an intrinsic property (the gel of **3** was not chosen due its opaque appearance). Images from both the bright-field and fluorescence microscopy concur with the observed FESEM of **4**−**6**, indicating an intertwined fibrous network for **4** while a porous three-dimensional (3D) network is seen for **5** and **6**, respectively.

Circular Dichroism. The supramolecular chirality originated from the chiral monomer during the process of gelation was measured by taking the CD spectra of gelator **6.** A strong negative Cotton effect at 228 nm ($\pi-\pi^*$) and a weak broad positive Cotton effect at 248−307 nm ($n-\pi^*$) indicate the

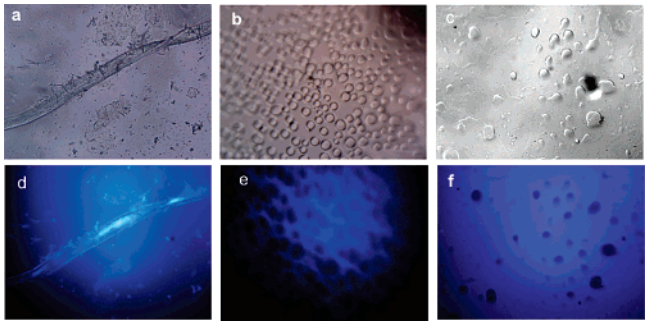

Figure 3. (a−c) Light microscopic images and (d−f) fluorescence microscopic images of the hydrogel of **4**−**6** at MGC.

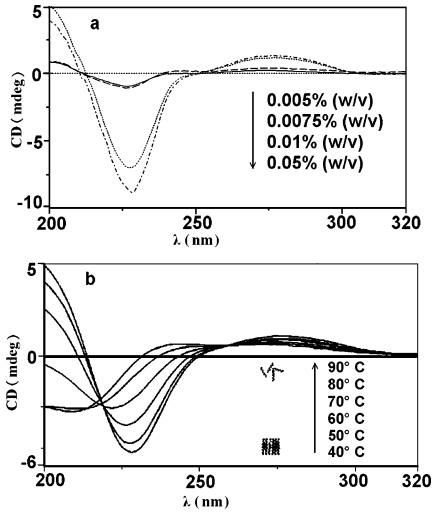

Figure 4. (a) CD spectra of **6** in plain water with varying concentration from 0.005 to 0.05% (w/v) at room temperature. (b) CD spectra of **6** at 0.05% (w/v) in plain water with varying temperature from 40 to 90 °C.

probable chiral helical arrangement of **6** (Figure 4a).[32−36] An increase in negative Cotton effect at 228 nm with gelator concentration also suggests highly ordered chiral planes at the supramolecular level induced by the dipeptide residues. Furthermore, development of supramolecular helicity emerged through noncovalent organized packing of molecular components in the process of self-aggregation was investigated by the temperature-dependent CD spectrum of gelator **6** from 40 to 90 °C at 0.05% (w/v; Figure 4b). With an increase in temperature the intensity at 228 nm due to the Cotton effect steadily decreased, implying the loss of supramolecular chirality. The molecules have lost their positional order while changing the physical status from gel to solution with a rise in temperature.[34] Hence, the observed CD intensity at the gel state is due to supramolecular aggregates not due to the molecular chirality.

^{1}H NMR Experiment. To get a quantitative idea on the orientation of the gelator molecule in the self-assembled 3D network primarily due to noncovalent interactions at the molecular level of individual gelator, a systematic NMR study was performed using 1% (w/v) of the most efficient gelator **6** with varying water content.[30,37−40] The indole N−H (H_a) as well as two amide protons (H_b and H_c, Scheme 1) of **6** showed an upfield shift with an increase in the water content from 10 to 50% (Figure 5a). The amide N−H_b shifted upfield from 8.71 to 8.53 ppm as the water content increased from 0 to 20%, and then remained almost constant over 8.53 ppm up to 40% water content. It again shifted to upfield to 8.44 ppm at 50% water. The observed upfield shift of H_a with increased water content from 10.85 to 10.31 ppm may be due to replacement of

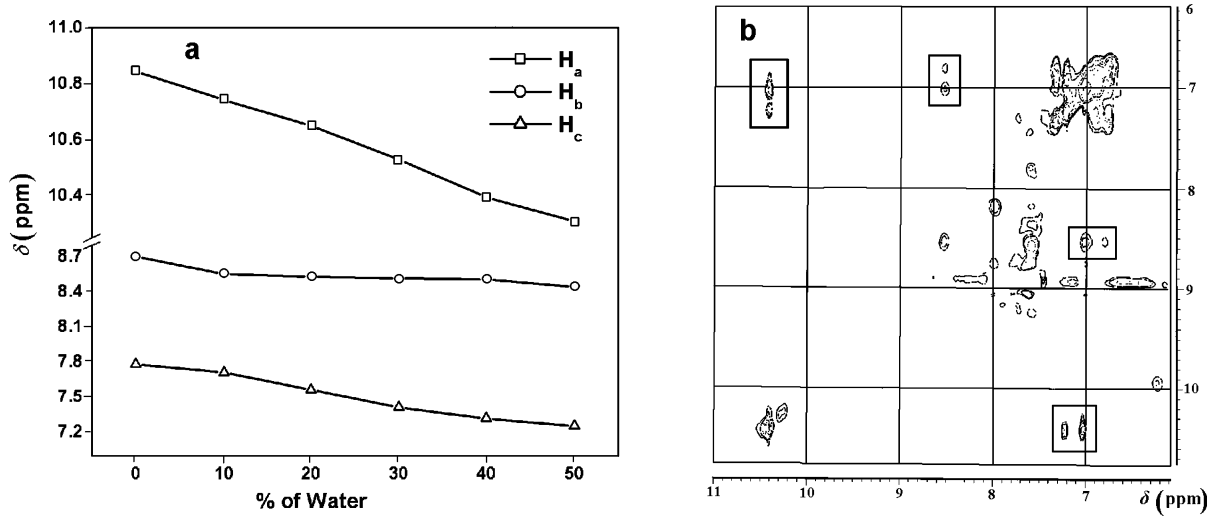

Figure 5. (a) Change in ^{1}H NMR chemical shift of **6** (1%, w/v) in [D_6]DMSO with varying H_2O content; (b) 2D-NOESY spectra of 1% (w/v) **6** gelator in [D_6]DMSO with 40% water.

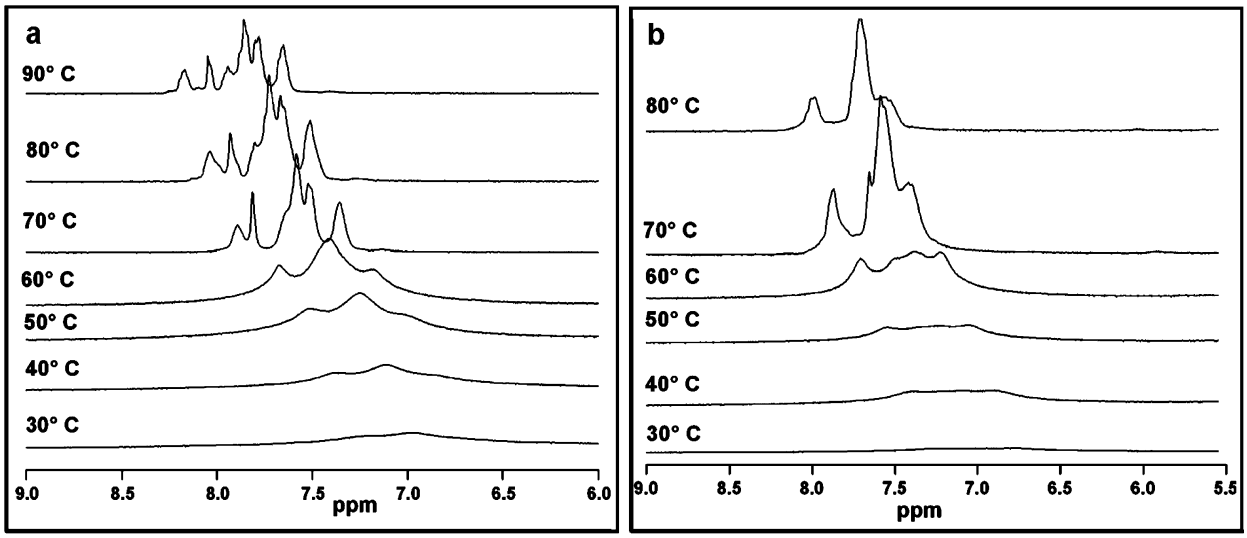

Figure 6. ^{1}H NMR spectra of transparent hydrogel, **5** and **6** (1%, w/v, a and b, respectively), in D_2O with varying temperature from 30 to 90 °C.

intermolecular hydrogen bonding between [D_6]DMSO (−S═O---H_a—N) with H_2O (H_2O---H_a—N). Also upon initiation of the self-assembling process with increasing water content, the bulky indole group presumably twisted toward the hydrophobic domain of the self-aggregate, thereby exposing the carbonyl group in the aqueous phase.[37] Such changes in orientation of the gelator molecule possibly confine the amide and indole N−H in the hydrophobic region resulting in an upfield shift of both protons. While within 20−40% water content amide N−H_b possibly starts participating in the intermolecular hydrogen bonding with the carbonyl oxygen that may lead to local dehydration around this proton. Consequently that would initiate the formation of a fibrous network and also is expected to result in the downfield shift of amide proton. However, the continuous shielding effect because of the increasing water at the head group region and the development of the hydrophobic domain as a result of increased $\pi-\pi$ interaction between the parallel aromatic rings competes with the deshielding effect resulting in almost no change in the chemical shift of amide protons within 20−40% water content. The influence of the $\pi-\pi$ interaction induced hydrophobic domain on gelation was further confirmed from a temperature-dependent ^{1}H NMR study of efficient hydrogels, **5** and **6** (1%, w/ v) in D_2O (Figure 6). In the gel state at 30 °C a broad peak is seen for aromatic protons, which are very much shielded due to possible $\pi-\pi$ stacking between the aromatic moieties in the self-aggregated form. As the temperature increases, the intermolecular hydrogen bonding gets destroyed, leading to the phase transition from gel to sol, where the spinning nuclei show their characteristic signal. Also the rise in temperature removes the hydrophobic stacking resulting in downfield shift (∼6.72 to 8.16 ppm) of aromatic protons. The temperature (∼70 °C) at which the splitting of protons for 5 and 6 was observed is comparable to those of protons signals at ∼70 °C (Figure 6) for **5** and **6** are comparable to those of T_{gel} values of both the gelator at 1% (w/v) deduced from T_{gel} and the gelator concentration (Figure 1). Besides the contribution of both amide and indole N−Hs, the $\pi-\pi$ interaction plays an important role in gelation mechanism through the development of hydrophobic domain.

In continuation with the preceding observation we did further investigation on the possible intermolecular interactions between gelator and its neighbor molecules using 2D NOESY experiments with **6** (1.0%, w/v) in [D_6]DMSO and also in the presence of 40% water. As expected, no off-diagonal cross-peak was observed at the nongelated state of the amphiphiles in [D_6]DMSO. At 40% water content, (Figure 5b) off-diagonal cross-peaks were observed between the aromatic rings and N−Hs of indole and amides. This observation clearly specifies

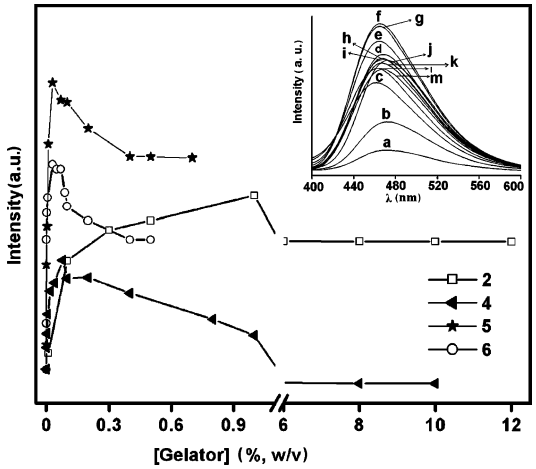

Figure 7. Luminescence spectra of ANS (1×10^{-5} M) with varying concentrations of gelator in water at room temperature. Concentrations: for **2**, 0.01, 0.1, 0.3, 0.5, 1, 3, 6, 8, 10, and 12% (w/v); for **4**, 2×10^{-4}, 0.002, 0.004, 0.008, 0.02, 0.04, 0.08, 0.1, 0.2, 0.4, 0.8, 1, 2, 3, 5, 8, and 10% (w/v); for **5**, 3×10^{-4}, 5×10^{-4}, 0.003, 0.005, 0.01, 0.03, 0.07, 0.1, 0.2, 0.4, 0.5, and 0.7% (w/v); for **6**, 3×10^{-4}, 5×10^{-4}, 1×10^{-3}, 0.003, 0.007, 0.03, 0.05, 0.07, 0.09, 0.1, 0.2, 0.4, and 0.5% (w/v). Inset: the representative fluorescence spectra of ANS in **6** with increasing concentration (as said above) from a to m.

that a strong interaction exists between the protons of N−Hs and the aromatic ring through space that plays the crucial role in gelation. Such observation is consistent with the upfield shift of N−H protons with increasing water content in [D_6]DMSO observed in 1D-NMR study. The absence of any long-range interactions in only [D_6]DMSO additionally complement the obvious contribution of N−H$\cdots\pi$ interaction in gelation.[29,30]

Luminescence Study. As mentioned in the preceding paragraphs, hydrophobic interaction is the major driving force toward controlling the hydrogelation; it was further probed by taking luminescence spectra of 8-anilino-1-naphthalenesulphonic acid (ANS), the popular hydrophobic fluorescence probe, during the hydrogelation (transparent) of **2** and **4**−**6** (Figure 7). With an increase in gelator concentration, the ANS intensity at first rapidly increases to a maximum with the blue shift from 510 (in plain water) to ∼465 nm. After that a slow decrease was observed with a slight red shift of ∼4 nm; then it became almost constant with no change in the emission intensity. The steady intensity was observed at a concentration which is ∼10 times lower than the MGC of the corresponding gelators showing their propensity to aggregate further into nanofibers as observed in microscopic and CD study. Surprisingly, transparent gels of **2**/**4** and **5**/**6** have similar fluorescence behavior. The intensity values for **2**/**4** are lower than those for the **5**/**6** gel pair at comparable concentrations, indicating the involvement of a greater hydrophobic domain in the self-assembling process of the later pair compared to the former. This might be due to the rigid/strained proline moiety in **2**/**4** that hinders the desired planar supramolecular arrangement in the gel state leading to the development of a less hydrophobic domain and consequently higher MGC (Table 1), while incorporation of a planar aromatic moiety in **5**/**6** forms a pocket that is more hydrophobic in nature and can hold more interstitial water yielding low MGC. However, in all the cases at the gel state the molecules are aligned in a well-ordered network and experience a less hydrophobic environment compared to that of the intermediate state of gelation. Thus, gelation processes seem to undergo via an intermediate state of self-assembly[41] to which ANS has a higher binding affinity compared to that at the gel state. The preceding behavior of ANS is a distinct feature of the existence of a hydrophobic environment indicating its participation in hydrogelation.

TABLE 2: FTIR Spectroscopic Data[a] for the Gelators in $CHCl_3$ and in D_2O at MGC

FTIR absorption band	2		4		5		6	
	$CHCl_3$	D_2O	$CHCl_3$	D_2O	$CHCl_3$	D_2O	$CHCl_3$	D_2O
amide I	1687	1650	1676	1647	1670	1652	1681	1654
amide II	1531	1558	1529	1552	1525	1539	1521	1553

[a] Values are given in cm^{-1}.

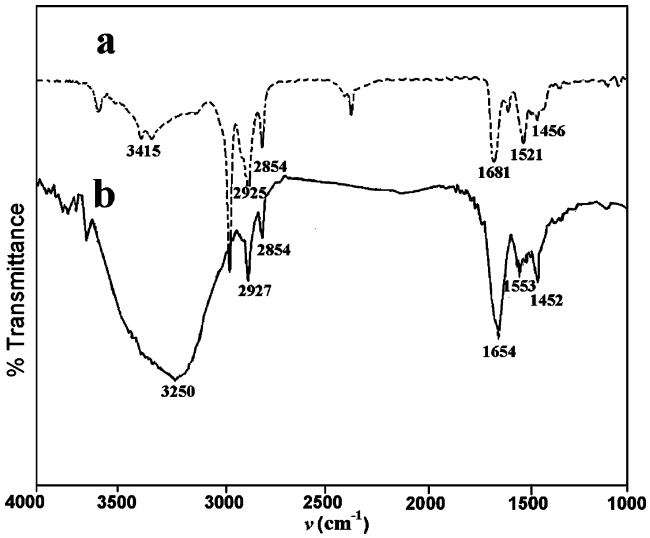

Figure 8. Representative FTIR spectra of the gelator **6** in $CHCl_3$ (a) and D_2O (b) at MGC (0.25%, w/v).

FTIR Spectroscopy. To establish the involvement of intermolecular hydrogen bonding between amide N−H and carbonyl oxygen in the gelation process as revealed in the ^{1}H NMR study, FTIR spectroscopy was performed for all the transparent gels and their solution state. As it is impossible to extract information on intermolecular interaction in hydrogelation from FTIR spectra in H_2O, we have taken the spectra of dehydrated transparent hydrogels in D_2O and non-self-assembled species in $CHCl_3$ (Table 2).[26,27,42−47] The absorption frequencies in dried gels are always lower for the C═O stretching band (amide I) and higher for the N−H bending band (amide II) compared to that in $CHCl_3$.[43] The FTIR spectrum of **2** and **4**−**6** in $CHCl_3$ demonstrates the transmission bands at 1670−1687 cm^{-1} (ν(C═O), amide I) and 1521−1531 cm^{-1} (δ(N−H), amide II) assigned to the non-hydrogen bonding amide group, while in D_2O, the transmission bands at 1647−1654 cm^{-1} (amide I), 1539−1558 cm^{-1} (amide II), and a broad amide N−H band around 3203−3270 cm^{-1} characterized the hydrogen bonded amide groups (Figure 8, representative spectra of **6**). Also, an increase in intensity of the methylene scissoring vibration $\delta(CH_2)$ band ∼1460 cm^{-1} for **6** (Figure 8) in D_2O indicates the high trans conformational packing of the alkyl chain.[26,27] Again on gelation, the intensity of the amide II reduces, indicating enhanced rigidity within the gel network. Thus, the FTIR study illustrates the participation of hydrogen bonding as well as van der Waals interactions between the interconnected molecules in the formation of an entangled fibrous network on gelation.

Overall, the structure elucidation by spectroscopic and microscopic studies delineate that the self-assembling process involves intermolecular hydrogen bonding, $\pi-\pi$ stacking, N−H$\cdots\pi$ and hydrophobic interactions leading to the formation

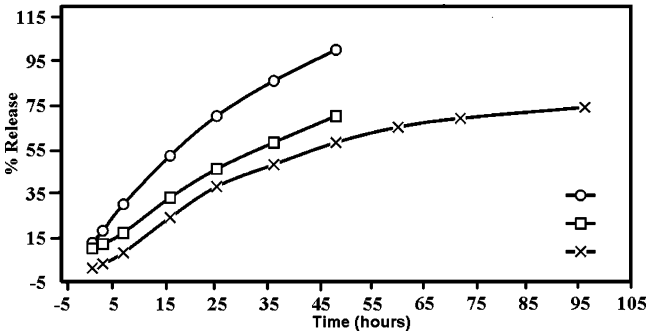

Figure 9. Controlled release of vitamin B_6 from hydrogel **6** at 0.5%, w/v (○), 3.0%, w/v (□), and vitamin B_{12} from **6** at 3.0%, w/v (×) with time at room temperature.

of entangled, helical, porous nanofibers, which in turn produce the hydrogel.

Controlled Release Study. It has been elucidated from earlier literature that gels made up in plain water, an intrinsic constituent of nature, have immense application as a potent delivery vehicle for biomolecules such as enzymes and proteins etc. In this context, the observed porosity in SEM and TEM images of the most efficient hydrogelator, **6**, motivated us to explore the possible use of this hydrogel in drug delivery as prospective biomedicinal applications. Bio-inspired nanocages of **6** were used to entrap hydrophilic biomolecules of different mass, vitamins B_6 and B_{12}, which got released in plain water without any additives and chemical modification in a controlled manner with time.[48−52] The release study was quantitatively determined by UV−vis spectrophotometer. Vitamin B_6 released faster 100 and 70%, respectively, from 0.5% than 3.0% (w/v) gel in 48 h, while vitamin B_{12} released slowly (74% in 96 h) from 3.0% (w/v) gel (Figure 9). These data clearly showed that vitamin B_6, the smaller biomolecule (lower mass) of the two used, was released from the gel with a typical diffusion behavior. Vitamin B_{12}, the larger one, probably confined in the hydrophobic domain of the 3D gel matrix, took a longer time to get released from the hydrogel.

Conclusion

Herein we have systematically analyzed the hydrogelation property of cationic peptide amphiphiles with special emphasis on the structural aspects as well as the mechanism of the gelation processes. The gelation process was understood at the molecular level to explain how minute changes in the chemical structure influence the self-assembling mechanism. The hydrogels were successfully used as hosts for controlled release of biomolecules. The present hydrogelators are expected to be very potent for antimicrobial activity due to the excellent cell membrane penetration ability of positively charged quaternary ammonium amphiphiles.[53−57] Further work will focus on the potential use of these hydrogels in encapsulating and releasing various bioactive agents and also on their antibacterial efficiency and cytotoxicity to mammalian cells for various potential biomedicinal applications.

Acknowledgment. D.D. and S.R. acknowledge CSIR, India for their Research Fellowships, and P.K.D. is thankful to the Department of Science and Technology, Government of India, for financial assistance through the Ramanna Fellowship.

Supporting Information Available: Synthesis and characterization of the peptide amphiphiles and TEM images of a dried gel of **6** at MGC. This material is available free of charge via the Internet at http://pubs.acs.org.

References and Notes

(1) Chirila, T. V.; Constable, I. J.; Crawford, G. J.; Vijayasekaran, S.; Thompson, D. E.; Chen, Y.-C.; Fletcher, W. A.; Griffin, B. J. *Biomaterials* **1993**, *14*, 26−38.
(2) Tabata, Y.; Ikada, Y. *Adv. Drug Delivery Rev.* **1998**, *31*, 287−301.
(3) Nishikawa, T.; Akiyoshi, K.; Sunamoto, J. *Macromolecules* **1994**, *27*, 7654−7659.
(4) Chu, Y. H.; Chen, J. K.; Whitesides, G. M. *Anal. Chem.* **1993**, *65*, 1314−1322.
(5) Lee, K.; Asher, S. A. *J. Am. Chem. Soc.* **2000**, *122*, 9534−9537.
(6) Estroff, L. A.; Hamilton, A. D. *Angew. Chem., Int. Ed.* **2000**, *39*, 3447−3450.
(7) Estroff, L. A.; Leiserowitz, L.; Addadi, L.; Weiner, S.; Hamilton, A. D. *Adv. Mater.* **2003**, *15*, 38−42.
(8) Bieser, A. M.; Tiller, J. C. *Chem. Commun. (Cambridge)* **2005**, 3942−3944.
(9) John, G.; Vemula, P. K. *Soft Matter* **2006**, *2*, 909−914.
(10) Vemula, P. K.; Li, J.; John, G. *J. Am. Chem. Soc.* **2006**, *128*, 8932−8938.
(11) Tiller, J. C. *Angew. Chem., Int. Ed.* **2003**, *42*, 3072−3075.
(12) Bhattacharya, S.; Srivastava, A.; Pal, A. *Angew. Chem., Int. Ed.* **2006**, *45*, 2934−2937.
(13) George, S. J.; Ajayaghosh, A.; Jonkheijm, P.; Schenning, A. P. H. J.; Meijer, E. W. *Angew. Chem., Int. Ed.* **2004**, *43*, 3422−3425.
(14) Sangeetha, N. M.; Maitra, U. *Chem. Soc. Rev.* **2005**, *34*, 821−836.
(15) Jayawarna, V.; Ali, M.; Jowitt, T. A.; Miller, A. E.; Saiani, A.; Gough, J. E.; Ulijn, R. V. *Adv. Mater.* **2006**, *18*, 611−614.
(16) Yang, Y.; Suzuki, M.; Owa, S.; Shirai, H.; Hanabusa, K. *J. Am. Chem. Soc.* **2007**, *129*, 581−587.
(17) Vemula, P. K.; John, G. *Chem. Commun. (Cambridge)* **2006**, 2218−2220.
(18) van Esch, J.; Feringa, B. L. *Angew. Chem., Int. Ed.* **2000**, *39*, 2263−2266.
(19) Estroff, L. A.; Hamilton, A. D. *Chem. Rev.* **2004**, *104*, 1201−1217, and references therein.
(20) van Bommel, K. J. C.; van der Pol, C.; Muizebelt, I.; Friggeri, A.; Heeres, A.; Meetsma, A.; Feringa, B. L.; van Esch, J. *Angew. Chem., Int. Ed.* **2004**, *43*, 1663−1667.
(21) Lee, K. Y.; Mooney, D. J. *Chem. Rev.* **2001**, *101*, 1869−1880.
(22) Wang, G.; Hamilton, A. D. *Chem. Commun. (Cambridge)* **2003**, 310−311.
(23) Bhuniya, S.; Park, S. M.; Kim, B. H. *Org. Lett.* **2005**, *7*, 1741−1744.
(24) Beebe, D. J.; Moore, J. S.; Bauer, J. M.; Liu, Q. Yu, R. H.; Devadoss, C.; Jo, B. H. *Nature* **2000**, *404*, 588−590.
(25) Bhuniya S.; Seo, Y. J.; Kim, B. H. *Tetrahedron Lett.* **2006**, *47*, 7153−7156.
(26) Kogiso, M.; Hanada, T.; Yase, K.; Shimizu, T. *Chem. Commun. (Cambridge)* **1998**, 1791−1792.
(27) Köhler, K.; Förster, G.; Hauser, A.; Dobner, B.; Heiser, U. F.; Ziethe, F.; Richter, W.; Steiniger, F.; Drechsler, M.; Stettin, H.; Blume, A. *J. Am. Chem. Soc.* **2004**, *126*, 16804−16813.
(28) Menger, F. M.; Caran, K. L. *J. Am. Chem. Soc.* **2000**, *122*, 11679−11691.
(29) Takahasi, A.; Sakai, M.; Kato, T. *Polym. J.* **1980**, *12*, 335−341. Mukhopadhyay, S.; Maitra, U.; Krishnamoory, I. G.; Schmidt, J.; Talmon, Y. *J. Am. Chem. Soc.* **2004**, *126*, 15905−15914.
(30) (a) Das, D.; Dasgupta, A.; Roy, S.; Mitra, R. N.; Debnath, S.; Das, P. K. *Chem. Eur. J.* **2006**, *12*, 5068−5074. (b) Roy, S.; Dasgupta, A.; Das, P. K. *Langmuir* **2007**, *23*, 11769.
(31) (a) Dasgupta, A.; Mitra, R. N.; Roy, S.; Das, P. K. *Chem. Asian J.* **2006**, *1*, 780−788. (b) Roy, S.; Das, D.; Dasgupta, A.; Mitra, R. N.; Das, P. K. *Langmuir* **2005**, *21*, 10398−10404.
(32) Gratzer, W. B.; Holzwarth, G. M.; Doty, P. *Proc. Natl. Acad. Sci. U.S.A.* **1961**, *47*, 1785−1791.
(33) Zhang, Y.; Yang, H.; Gu, Z.; Xu, B. *J. Am. Chem. Soc.* **2003**, *125*, 13680−13681.
(34) Friggeri, A.; Pol, C. V. D.; Bommel, K. J. C. V.; Heeres, A.; Stuart, M. C. A.; Feringa, B. L.; van Esch, J. *Chem. Eur. J.* **2005**, *11*, 5353−5361.
(35) Yang, Z.; Liang, G.; Ma, M.; Gao, Y.; Xu, B. *J. Mater. Chem.* **2007**, *17*, 850−854.
(36) Yang, Z.; Lianga, G.; Xu, B. *Chem. Commun. (Cambridge)* **2006**, 738−740.
(37) Billiot, F. H.; McCarroll, M.; Billiot, E. J.; Rugutt, J. K.; Morris, K.; Warner, I. M. *Langmuir* **2002**, *18*, 2993−2997.
(38) Suzuki, M.; Yumoto, M.; Kimura, M.; Shirai, H.; Hanabusa, K. *Chem. Eur. J.* **2003**, *9*, 348−354.
(39) Yang, Z.; Xu, K.; Wang, L.; Gu, H.; Wei, H.; Zhang, M.; Xu, B. *Chem. Commun. (Cambridge)* **2005**, 4414−4416.

(40) Schoonbeek, F. S.; van Esch, J. H.; Hulst, R.; Kellogg, R. M.; Feringa, B. L. *Chem. Eur. J.* **2000**, *6*, 2633−2643.
(41) Maitra, U.; Mukhopadhyay, S.; Sarkar, A.; Rao, P.; Indi, S. S. *Angew. Chem., Int. Ed.* **2001**, *40*, 2281−2283.
(42) Jung, J. H.; Shinkai, S.; Shimizu, T. *Chem. Eur. J.* **2002**, *8*, 2684−2690.
(43) Shimizu, T.; Masuda, M. *J. Am. Chem. Soc.* **1997**, *119*, 2812−2818.
(44) Yamada, N.; Ariga, K.; Naito, M.; Matsubara, K.; Koyama, E. *J. Am. Chem. Soc.* **1998**, *120*, 12192−12199.
(45) Jung, J. H.; John, G.; Masuda, M.; Yoshida, K.; Shinkai, S.; Shimizu, T. *Langmuir* **2001**, *17*, 7229−7232.
(46) deLoos, M.; Friggeri, A.; van Esch, J.; Kellogga, R. M.; Feringa, B. L. *Org. Biomol. Chem.* **2005**, *3*, 1631−1639.
(47) Suzuki, M.; Sato, T.; Kurose, A.; Shiraib, H.; Hanabusa, K. *Tetrahedron Lett.* **2005**, *46*, 2741−2745.
(48) Vinogradov, S. V.; Bronich, T. K.; Kabanov, A. V. *Adv. Drug Delivery Rev.* **2002**, *54*, 135−147.
(49) Friggeri, A.; Feringa, B. L.; van Esch, J. *J. Controlled Release* **2004**, *97*, 241−248.
(50) Zhou, S. L.; Matsumoto, S.; Tian, H. D.; Yamane, H.; Ojida, A.; Kiyonaka, S.; Hamachi, I. *Chem. Eur. J.* **2005**, *11*, 1130−1136.
(51) Mahler, A.; Reches, M.; Rechter, M.; Cohen, S.; Gazit, E. *Adv. Mater.* **2006**, *18*, 1365−1370.
(52) Murthy, N.; Thng, Y. X.; Schuck, S.; Xu, M. C.; Frechet, J. M. J. *J. Am. Chem. Soc.* **2002**, *124*, 12398−12399.
(53) Dizman, B.; Elasri, M. O.; Mathias, L. J. *J. Appl. Polym. Sci.* **2004**, *94*, 635−642.
(54) Coessens, V.; Schacht, E.; Domurado, D. *J. Controlled Release* **1997**, *47*, 283−291.
(55) Yang, M.; Santerre, J. P. *Biomacromolecules* **2001**, *2*, 134−141.
(56) Dizman, B.; Elasri, M. O.; Mathias, L. J. *Biomacromolecules* **2005**, *6*, 514−520.
(57) Ikeda, T.; Yamaguchi, H.; Tazuke, S. *Antimicrob. Agents Chemother.* **1984**, *26*, 139−144.